DOI: 10.1002/ejic.200900983

The *closo*-$[Sn_9Ir(cod)]^{3-}$ and $[Pb_9Ir(cod)]^{3-}$ Zintl Ions: Isostructural Ir^I Derivatives of the *nido*-E_9^{4-} Anions (E = Sn, Pb)

Domonique O. Downing,[a] Peter Zavalij,[a] and Bryan W. Eichhorn*[a]

Keywords: Zintl anions / Cluster compounds / Structure elucidation / Charge transfer / Solid-state structures

The *closo*-$[E_9Ir(cod)]^{3-}$ ions where E = Sn (**1**), Pb (**2**) (cod = 1,5-cyclooctadiene) were prepared from precursors $[Ir(cod)Cl]_2$, K_4E_9, and 2,2,2-cryptand in ethylenediamine/toluene solvent mixtures. The $[K(2,2,2\text{-crypt})]^+$ salts were isolated and characterized by NMR spectroscopy and single-crystal X-ray diffraction. The clusters are the first known Ir^I Zintl clusters and are examples of isostructural Sn/Pb homologues. Complexes **1** and **2** have 22-electron, bicapped square-antiprismatic structures and pseudo-C_{4v} point symmetry with the Ir(cod) vertices attached in an η^4 fashion. The structural studies and ^1H and ^{13}C NMR spectroscopic studies showed significant charge transfer to the COD ligands.

Introduction

Bimetallic clusters derived from the E_9^{4-} Zintl ions (E = Ge, Sn, Pb) are of interest due to their unique structures and properties as well as their similarity to fullerenes.[1] Particularly interesting is the ability for both fullerenes and Zintl clusters to form endohedral structures[1,2] in which the centered elements are in highly symmetric coordination geometries (e.g. the I_h symmetries of La and Pt in La@C_{60} and $[Pt@Pb_{12}]^{2-}$).[3,4] Numerous endohedral Zintl clusters have been synthesized from the $E_9^{3-/4-}$ ions where E = Ge, Sn, Pb. Examples include $[M@Pb_{10}]^{2-}$ and $[M@Pb_{12}]^{2-}$ (M = Ni, Pd, Pt), $[Cu@E_9]^{3-}$ (E = Sn, Pb), $[Sn_9Pt_2(PPh_3)]^{2-}$, and $Pd_2@E_{18}{}^{2-}$ (E = Ge, Sn).[3,5–9] While 9-vertex and 10-vertex clusters are known with and without endohedral atoms, structures with more than 10 vertices are expected to have interstitial atoms when prepared in solution or the solid state.[1] All of these complexes can be described as derivatives of Wade–Mingos type deltahedral clusters with the exception of the recent theoretical and experimental results showing the remarkable non-deltahedral structures in the D_{5h}-$[M@Ge_{10}]^{3-}$ complexes (M = Co, Fe).[10–13] Korber noted[13] that these structures might mark the emergence of a new class of fullerene-like clusters based on fused pentagonal rings as is predicted to exist in the Hf@Ge_n series.[13,14]

To further develop the area of group 8 and 9 transition-metal derivatives of the Zintl clusters, we have been studying the reactions of labile Ir complexes with Sn_9^{4-} and Pb_9^{4-}. Herein we report the synthesis of the ions $[Sn_9Ir(cod)]^{3-}$ and $[Pb_9Ir(cod)]^{3-}$ (cod = 1,5-cyclooctadiene). Both clusters possess a C_{4v}-type *closo*-deltahedral structure with 22 electrons and are diamagnetic. The clusters described herein are the first Ir–Sn and Ir–Pb bimetallic clusters and are examples of homologous Sn-Pb transition-metal derivatives.

Results

Synthesis

Ethylenediamine (en) solutions of K_4Sn_9 and K_4Pb_9 react with toluene (tol) solutions of $[Ir(cod)Cl]_2$ in the presence of 2,2,2-crypt to give the $[Sn_9Ir(cod)]^{3-}$ and $[Pb_9Ir(cod)]^{3-}$ ions, respectively [Equation (1)]. The $[K(2,2,2\text{-crypt})]^+$ salts were isolated in ca. 30% yield.

$$2\,E_9^{4-} + [Ir(cod)Cl]_2 \xrightarrow{(2.2.2\text{-crypt})} 2\,[E_9Ir(cod)]^{3-} + 2\,Cl^- \qquad E = Sn\ (\mathbf{1}),\ Pb\ (\mathbf{2}) \qquad (1)$$

The $[K(2,2,2\text{-crypt})]^+$ salts of both clusters are air and moisture sensitive in solution and in the solid state. The salts are soluble in pyridine and DMF and have been characterized by single-crystal X-ray diffraction and ^1H NMR and ^{13}C NMR spectroscopy.

Solid-State Structures

The $[K(2,2,2\text{-crypt})]_3[E_9Ir(cod)]$ salts (E = Sn, Pb) are triclinic, space group $P\bar{1}$, and are isomorphic. Selected bond lengths and angles for $[Sn_9Ir(cod)]^{3-}$ and $[Pb_9Ir(cod)]^{3-}$ are given in Table 1 and 2, respectively. Two views of the clusters are shown in Figure 1.

The structure of anion **1** contains a bicapped square antiprism in which the Ir and Sn(1) atoms occupy capping sites and are bound to four Sn atoms. The remaining eight Sn

---

[a] Department of Chemistry and Biochemistry, University of Maryland,
College Park, MD 20742, USA

Supporting information for this article is available on the WWW under http://dx.doi.org/10.1002/ejic.200900983.

Table 1. Selected bond lengths [Å] and angles [°] for the $[Sn_9Ir(cod)]^{3-}$ ion.

Ir(1)–Sn(6)	2.7800(4)	Sn(5)–Sn(8)	2.9887(5)
Ir(1)–Sn(7)	2.7654(5)	Sn(5)–Sn(9)	2.9805(6)
Ir(1)–Sn(8)	2.7735(4)	Sn(6)–Sn(7)	3.1102(5)
Ir(1)–Sn(9)	2.7629(4)	Sn(6)–Sn(9)	3.1067(5)
Sn(1)–Sn(2)	2.9575(7)	Sn(7)–Sn(8)	3.1162(5)
Sn(1)–Sn(3)	2.9609(6)	Sn(8)–Sn(9)	3.1067(5)
Sn(1)–Sn(4)	2.9258(6)	Ir(1)–C(1)	2.139(6)
Sn(1)–Sn(5)	2.9549(6)	Ir(1)–C(2)	2.156(7)
Sn(2)–Sn(3)	3.0971(6)	Ir(1)–C(5)	2.146(6)
Sn(2)–Sn(5)	3.2072(6)	Ir(1)–C(6)	2.156(6)
Sn(2)–Sn(6)	2.9950(6)	C(1)–C(2)	1.419(10)
Sn(2)–Sn(9)	3.0003(5)	C(1)–C(8)	1.521(10)
Sn(3)–Sn(4)	3.1765(5)	C(2)–C(3)	1.534(9)
Sn(3)–Sn(6)	3.0073(6)	C(3)–C(4)	1.523(9)
Sn(3)–Sn(7)	2.9648(5)	C(4)–C(5)	1.501(9)
Sn(4)–Sn(5)	3.1239(6)	C(5)–C(6)	1.426(9)
Sn(4)–Sn(7)	2.9868(6)	C(6)–C(7)	1.522(10)
Sn(4)–Sn(8)	2.9873(5)	C(7)–C(8)	1.513(11)
C(1)–Ir(1)–C(2)	38.6(3)	C(1)–Ir(1)–Sn(8)	92.68(18)
C(1)–Ir(1)–C(5)	96.4(2)	C(2)–Ir(1)–Sn(8)	126.68(17)
C(5)–Ir(1)–C(2)	79.9(2)	C(5)–Ir(1)–Sn(8)	139.90(18)
C(1)–Ir(1)–C(6)	79.9(3)	C(6)–Ir(1)–Sn(8)	105.91(18)
C(5)–Ir(1)–C(6)	38.7(2)	Sn(9)–Ir(1)–Sn(6)	67.105(12)
C(2)–Ir(1)–C(6)	88.4(3)	Sn(3)–Sn(2)–Sn(5)	90.101(15)
C(1)–Ir(1)–Sn(6)	137.1(2)	Sn(2)–Sn(3)–Sn(4)	90.375(14)
C(5)–Ir(1)–Sn(6)	93.61(17)	Sn(5)–Sn(4)–Sn(3)	90.185(15)
C(2)–Ir(1)–Sn(6)	103.64(19)	Sn(4)–Sn(5)–Sn(2)	89.331(14)
C(6)–Ir(1)–Sn(6)	128.49(18)	Sn(9)–Sn(6)–Sn(7)	89.235(14)
C(1)–Ir(1)–Sn(9)	85.49(18)	Sn(6)–Sn(7)–Sn(8)	90.661(14)
C(5)–Ir(1)–Sn(9)	151.25(18)	Sn(9)–Sn(8)–Sn(7)	88.349(13)
C(2)–Ir(1)–Sn(9)	84.12(18)	Sn(6)–Sn(9)–Sn(8)	91.720(14)
C(6)–Ir(1)–Sn(9)	164.11(18)	Sn(2)–Sn(1)–Sn(3)	63.108(15)

atoms make up the two square planes and are five coordinate in nature. According to Wade's rules,[15] the ion is a 10-vertex 22-electron *closo* deltahedron [each Sn = 2e⁻, (COD)Ir = 1e⁻, charge = 3e⁻]. The Ir–Sn bonds average 2.771(4) Å with a narrow range of 2.7629(4)–2.7800(4) Å. The Sn–Sn bonds are in the range 2.9258(6)–3.2072(6) Å, which is typical of Sn_9^{4-} derivatives, with the bonds of the η^4-Sn(1) having the shortest average bond length of 2.950(9) Å. The square antiprism is regular in nature (see Figure 1, b) as shown by the narrow distribution of the Sn–Sn–Sn bond angles in the square planes (90.0° ± 1.7°). The length of the diagonals Sn(6)–Sn(8) and Sn(7)–Sn(9) are 4.3981 Å and 4.3982 Å, respectively, giving them a ratio of 1.0. These data are indicative of a regular square antiprism containing pseudo C_{4v} symmetry.

The $[K(2,2,2\text{-crypt})]_3[Pb_9Ir(cod)]\cdot 2en$ crystals are isomorphic with the Sn analogue above although the crystals were weakly diffracting and did not provide a high quality structure. However, the connectivity is clear and the observed metric parameters are consistent with expectations. Due to the low quality of the structure, only the general features will be described here. The Ir–Pb bonds have a range of 2.844(3)–2.886(3) Å. The Pb–Pb bonds are in the range 3.043(4)–3.380(3) Å with the bonds of the η^4-Pb(1) having the shortest average bond length of 3.076(2) Å. The square antiprism is regular in nature as shown by the narrow distribution of the Pb–Pb–Pb bond angles in the square planes (90.0° ± 2.1°), with the square closer to the four coordinate Pb atom highly regular (90.0° ± 0.7°). The metric parameters are similar to those of $[Pb_9Mo(CO)_3]^{4-}$ and $[Pb_9Zn(C_6H_5)]^{3-}$.[8,16–18]

NMR Spectroscopy

The $^{13}C\{^1H\}$ NMR spectrum of the $[Pb_9Ir(cod)]^{3-}$ cluster (**2**) displays the resonances of crypt, the en solvates and residual toluene. The two COD signals appear at δ = 34.6 ppm and 70.6 ppm, which correspond to the methylene and olefinic carbon atoms A and B, respectively (Figure 2). The assignments were aided by observing the proton-coupled spectrum in which the methylene carbon split into a triplet [$^1J(^{13}C,^1H)$ = 123 Hz] and the alkenyl resonance split into a doublet [$^1J(^{13}C,^1H)$ = 151 Hz] of similar intensity. The latter is obscured in the $^{13}C\{^1H\}$ spectrum due to the similar chemical shift of the crypt resonance at δ = 70.5 ppm. Both resonances are deshielded relative to those of $[Ir(cod)Cl]_2$ at δ = 32.3 ppm and 62.2 ppm, respectively.

The ^{13}C NMR spectrum of $[Sn_9Ir(cod)]^{3-}$ in pyridine shows a methylene chemical shift of δ = 34.7 ppm, which is very similar to that of $[Pb_9Ir(cod)]^{3-}$. The second signal for A is obscured by the crypt resonance and has not been located.

Table 2. Bond lengths [Å] and ^{13}C NMR spectroscopic data of $[E_9Ir(cod)]^{3-}$ and additional Ir-cod complexes.[a]

	Ir–C [Å]	C=C [Å]	C–C [Å]	CH (ppm)	CH_2 (ppm)
$[Sn_9Ir(cod)]^{3-}$	2.150	1.423	1.520	–	34.7
$[Pb_9Ir(cod)]^{3-}$	–	–	–	70.6	34.6
[(hfac)Ir(cod)][21]	2.101	1.409	1.511	62.0	30.9
[Ir(1,4-κ-CH=C(Ph)CH=CPh)(cod)($NCCH_3$)(PMe_3)]BF_4[22]	2.306	1.369	1.520	–	–
[(cod)Ir(κ^2-*P*,*N*-indene)]⁺[23,24]	2.176	1.399	1.511	59.8, 93.4	28.8, 33.0
[(cod)Ir(κ^2-*P*,*N*-indene)][24]	–	–	–	54.6, 84.7	28.7, 32.8
[Ir(cod)(pyr)(PCy_3)]PF_6[25]	2.170	1.406	1.519	–	–
[NEt_3H][Ir(HL)(cod)][26]	2.115	1.428	1.513	–	–
[Ir(cod){$Ph_2Sb(CH_2)_3SbPh_2$}]BF_4[27]	–	–	–	63.8	36.5
[Ir(cod){o-$C_6H_4(CH_2SbMe_2)_2$}]BF_4[27]	–	–	–	59.2	33.6

[a] cod = 1,5-cycloocatdiene; hfac = 1,1,1,5,5,5-hexafluoroacetylacetonate; pyr = pyridine; cy = cyclohexyl; H_3L = 2,6-dioxo-1,2,3,6-tetrahydropyrimidine-4-carboxylic acid.

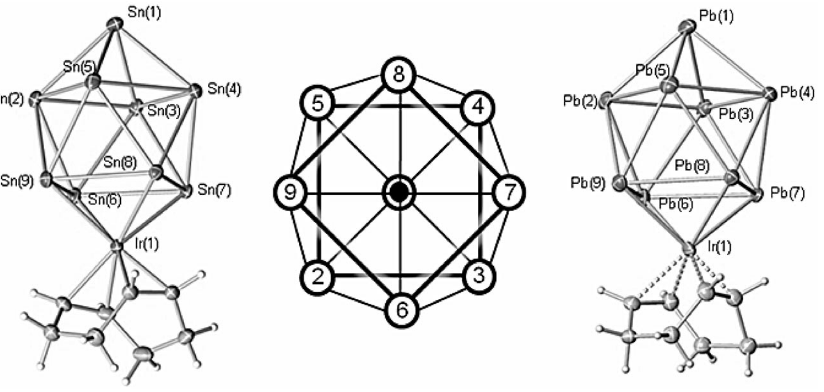

Figure 1. Drawings of the $[Sn_9Ir(cod)]^{3-}$ ion (**1**), showing (a) a side view and (b) a bottom view down the Sn(1)–Ir axis with the cod ligand omitted. (c) Drawing of the $[Pb_9Ir(cod)]^{3-}$ ion (**2**). Thermal ellipsoids drawn at the 50% probability level.

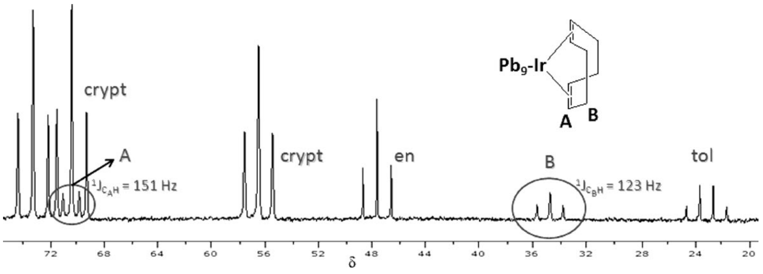

Figure 2. ^{13}C NMR spectrum for the $[K(2,2,2\text{-crypt})]_3[Pb_9Ir(cod)]\cdot 2en$ salt. Data were recorded at 300 K at 125.8 MHz in [D$_5$]pyridine.

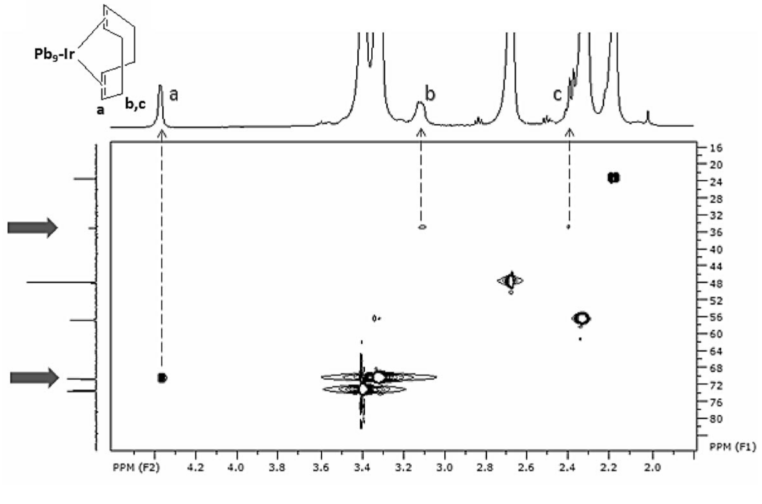

Figure 3. HSQC spectrum for the $[Pb_9Ir(cod)]^{3-}$ (**2**). Data was recorded at 300 K at 125.8 MHz in [D$_5$]pyridine.

The ^1H NMR spectrum for the $[K(2,2,2\text{-crypt})]_3[Pb_9Ir(cod)]\cdot 2en$ salt contains three signals for the $[Pb_9Ir(cod)]^{3-}$ cluster as expected. The olefinic proton, **a**, of the COD ligand has a chemical shift of δ = 4.38 ppm while the two diastereotopic protons, **b** and **c**, of the methylene carbon produce signals at δ = 2.38 and 3.11 ppm. Because the proton signals were broad, the chemical shifts and peak assignments were made through the use of the ^1H-^{13}C HSQC spectrum is shown in Figure 3.

Attempts to observe ^{119}Sn and ^{207}Pb NMR signals at various temperatures were unsuccessful despite the obvious diamagnetism of the compound.

Discussion

The $[Sn_9Ir(cod)]^{3-}$ and $[Pb_9Ir(cod)]^{3-}$ clusters described herein are the first Ir–Sn and Ir–Pb bimetallic clusters and are also examples of Sn–Pb homologues. Previous homologues include Fässler's [$Cu@Sn_9$]$^{3–}$ and [$Cu@Pb_9$]$^{3–}$ ions, the $E_9Mo(CO)_3{}^{4–}$ complexes,[16–18] and the *closo* clusters [$Sn_9M(Ar)$]$^{3–}$ and [$Pb_9M(Ar)$]$^{3–}$ where M = Zn, Cd; Ar = aryl, that also have silicon and germanium homologues.[8,19] The [$E_9Ir(cod)$]$^{3–}$ clusters described here are Wadian 10-vertex, 22-electron *closo* structures and are isostructural and isoelectronic to the $E_9M(CO)_3{}^{4–}$ series where M = Cr, Mo, W and to {$Ge_9[Si(SiMe_3)_3]_3Cr(CO)_3$}$^–$.[16–20]

It is informative to compare the [$E_9Ir(cod)$]$^{3–}$, [$Cu@E_9$]$^{3–}$ and [$E_9Zn(C_6H_5)$]$^{3–}$ clusters where E = Sn, Pb. While all three compounds can be viewed as $ML_n{}^+$ derivatives of the $E_9{}^{4–}$ parent, the Cu^+ ion occupies an interstitial site whereas the $Ir(COD)^+$ and $Zn(C_6H_5)^+$ units occupy vertex sites. However, in each case, the $ML_n{}^+$ units donate zero electrons to cluster bonding due to the fact that interstitial ions contribute valence electrons minus 10 $e^–$ and vertex units contribute valence electrons minus 12 $e^–$. As such, the Cu complexes are best viewed as 22-electron 9-vertex *nido*-$Cu@E_9{}^{3–}$ clusters whereas the [$E_9Ir(cod)$]$^{3–}$ and [$E_9Zn(C_6H_5)$]$^{3–}$ complexes form 22-electron 10-vertex *closo*-$E_9ML_n{}^{3–}$ structures. Interestingly, displacement of the neutral cod ligands from the [$E_9Ir(cod)$]$^{3–}$ clusters would give $E_9Ir^{3–}$ binary complexes, which would presumably have 20-electron *closo* structure with two fewer electrons than the $Cu@E_9{}^{3–}$ systems. Attempts to remove the COD ligands are in progress.

Information on the charge distribution in the [$E_9Ir(cod)$]$^{3–}$ complex can be discerned from examination of the carbon–carbon bond lengths of the cod ligands and their ^{13}C NMR chemical shifts. Formal π back bonding interactions between the occupied Ir d-orbitals and the C=C π* antibonding orbitals effectively weakens the C=C bonds of the cod ligands and lengthens the olefinic bond. Compared to other Ir^I-cod complexes listed in Table 2, the average C=C bond length is quite long at 1.423(4) Å and is comparable with the [Ir(2,6-dioxo-1,2,3,6-tetrahydropyrimidino-4-carboxylato)(cod)]$^{-1}$ anion.[26] In addition, the ^{13}C NMR chemical shift of the olefinic carbons are shifted downfield relative to those of typical cod ligands. Collectively, these data are indicative of significant charge transfer to the cod ligands and denote a highly activated C=C double bond.

Experimental Section

General: All reactions were preformed under nitrogen in a dry box. ^1H and ^{13}C NMR spectra were recorded with a Bruker DRX 500 AVANCE spectrometer operating at 500.1 MHz and 125.8 MHz respectively.

Chemicals: K_4Sn_9 and K_4Pb_9 were made by high-temperature fusion (ca. 1000 °C) of stoichiometric amounts of the elements. The chemicals were loaded into evacuated silica tubes and carefully heated with a natural gas/oxygen flame behind a blast shield. 4,7,13,16,21,24-Hexaoxa-1,10-diazobicyclo[8.8.8]hexacacosane (2,2,2-crypt) was purchased from Fisher Scientific. Bis(1,5-cyclooctadiene)diiridium(I) dichloride was purchased from Aldrich. Anhydrous ethylenediamine (en) and pyridine (pyr) were purchased from Fisher, vacuum distilled from K_4Sn_9, and stored under dinitrogen. Toluene was distilled from sodium/benzophenone under dinitrogen and stored under dinitrogen.

Preparation of [K(2,2,2-crypt)]$_3$[$Sn_9Ir(cod)$]·2en: In vial no. 1, K_4Sn_9 (73 mg, 0.056 mmol) was dissolved in en (ca. 2 mL), giving a dark red solution. Three equivalents of solid crypt (67 mg, 0.179 mmol) were added to the solution and allowed to stir for an hour. In vial 2, [$Ir(C_8H_{12})Cl$]$_2$ (20 mg, 0.030 mmol) was dissolved in toluene (ca. 2 mL) to produce an orange-yellow solution. The contents of vial no. 2 were slowly added to vial no. 1 and the reaction mixture was stirred for 2 h to yield a dark brown solution. The reaction mixture was then filtered through tightly packed glass wool in a pipet. Black crystals formed in the reaction vessel after 2 weeks (44 mg, 27% yield). ^{13}C NMR (125.8 MHz, [D_5]pyridine, 25 °C): δ = 34.7 ppm.

Preparation of [K(2,2,2-crypt)]$_3$[$Pb_9Ir(cod)$]·2en: In vial no. 1, K_4Pb_9 (179 mg, 0.089 mmol) was dissolved in en (ca. 4 mL), giving a dark red solution. Three equivalents of solid crypt (100 mg, 0.266 mmol) were added to the solution and allowed to stir for an hour. In vial 2, [$Ir(C_8H_{12})Cl$]$_2$ (30 mg, 0.044 mmol) was dissolved in toluene (ca. 4 mL) to produce an orange-yellow solution. The contents of vial no. 2 were slowly added to vial no. 1 and the reaction mixture was stirred for 2 h to yield a dark brown solution. The reaction mixture was then filtered through tightly packed glass wool in a pipet. Black crystals formed in the reaction vessel after 1 week (100 mg, 32% yield). ^1H NMR (500 MHz, [D_5]pyridine, 25 °C): δ = 2.38, 3.11, 4.38 ppm. ^{13}C NMR (125.8 MHz, [D_5]pyridine, 25 °C): δ = 34.6 [$^1J(^{13}C,^1H)$ = 123 Hz], 70.6 [$^1J(^{13}C,^1H)$ = 151 Hz].

Crystallographic Studies

[K(2,2,2-crypt)]$_3$[$Sn_9Ir(cod)$]·2en: A black crystal block (0.15 × 0.31 × 0.44 mm^3) was placed and optically centered on a Bruker Smart Apex II CCD system at –123 °C. The initial unit cell was indexed by using a least-squares analysis of a random set of reflections collected from three series of –0.3° in wide ω scans that were well distributed in reciprocal space. Data frames were collected [Mo-K_α] with –0.3° wide ω scans, 10 s per frame, with a crystal to detector distance of 5.200 cm, thus providing a complete sphere of data to $2\theta_{max}$ = 55°. A total of 64924 reflections were collected [22156 unique; R(int) = 0.0223] and corrected for Lorentz and polarization effects and absorption by using Blessing's method as incorporated into the program SADABS.

A summary of the crystallographic data is given in Table 3. The SHELXTL program package was implemented for data processing, structure solution, and refinement. System symmetry, lack of systematic absences, and intensity statistics indicated the centrosymmetric triclinic space group $P\bar{1}$. The structure was determined by direct methods with the successful location of the heavy atoms comprising the cluster. After several difference Fourier refinement cycles, all of the atoms were located, refined isotropically and then anisotropically. Disorder was found in one of the two ethylenediamine molecules in two orientations. Disorder also found in two of the three K-crypt$^+$ ions in a manner that cannot be modeled. Hydrogen atoms were placed in calculated positions. The final structure was refined to convergence [$\Delta/\sigma \leq 0.001$]. A final difference Fourier map was featureless indicating the structure is therefore both correct and complete.

[K(2,2,2-crypt)]$_3$[$Pb_9Ir(cod)$]·2en: A crystal plate (0.008 × 0.29 × 0.30 mm^3) was placed and optically centered on a Bruker Smart Apex II CCD system at –23 °C. The initial unit cell was indexed by using a least-squares analysis of a random set of reflections collected from three series of –0.3° in wide ω scans that were well distributed in reciprocal space. Data frames were collected [Mo-K_α] with –0.3° wide ω scans, 60 s per frame, with a crystal to detector distance of 5.200 cm, thus providing a complete sphere of data to $2\theta_{max}$ = 38°. A total of 15621 reflections were collected [10095

Table 3. Crystallographic data for $[K(2,2,2\text{-crypt})]_3[E_9Ir(C_8H_{12})]\cdot 2en$.

Empirical formula	$(C_8H_{12})IrSn_9\cdot 3(KC_{18}H_{36}N_2O_6)\cdot 2(C_2H_8N_2)$		$(C_8H_{12})IrPb_9\cdot 3(KC_{18}H_{36}N_2O_6)\cdot 2(C_2H_8N_2)$	
Formula weight	2735.56		3532.07	
Temperature	150(2) K		250(2) K	
Wavelength	0.71073 Å		0.71073 Å	
Crystal system	triclinic		triclinic	
Space group	$P\bar{1}$		$P\bar{1}$	
Unit cell dimensions	a = 14.8697(4) Å	α = 93.2366(5)°	a = 15.056(4) Å	α = 93.162(4)°
	b = 14.9149(4) Å	β = 93.1943(5)°	b = 15.218(4) Å	β = 93.921(4)°
	c = 23.6887(7) Å	γ = 112.5826(4)°	c = 24.045(6) Å	γ = 112.985(3)°
Volume	4826.0(2) Å^3		5039(2) Å^3	
Z	2		2	
Density, $\rho_{calcd.}$	1.883 g/cm^3		2.328 g/cm^3	
Absorption coefficient, μ	3.849 mm^{-1}		16.387 mm^{-1}	
Data/restraints/parameters	22156/120/1006		10095/1452/988	
Goodness-of-fit on F^2	1.000		0.934	
Final R indices: R_1,[a] $I > 2\sigma(I)$	0.0408		0.1184	
wR_2,[a] all data	0.0898		0.2353	

[a] $R_1 = \Sigma||F_o| - |F_c||/\Sigma|F_o|$, $wR_2 = [\Sigma w(F_o^2 - F_c^2)^2/\Sigma w(F_o^2)^2]^{1/2}$, $w = 1/[\sigma^2(F_o^2) + (0.02P)^2 + 35.1P]$.

unique; R(int) = 0.0797] and corrected for Lorentz and polarization effects and absorption by using Blessing's method as incorporated into the program SADABS.

A summary of the crystallographic data is given in Table 3. The SHELXTL program package was implemented for data processing, structure solution, and refinement. System symmetry, lack of systematic absences, and intensity statistics indicated the centrosymmetric triclinic space group $P\bar{1}$. The structure was determined by direct methods with the successful location of the heavy atoms comprising the cluster. After several difference Fourier refinement cycles, all of the atoms were located, refined isotropically and then anisotropically. Disorder was found in the organic species in the structure. Hydrogen atoms were placed in calculated positions. The final structure was refined to convergence [$\Delta/\sigma \leq 0.009$]. A final difference Fourier map was featureless indicating the structure is therefore both correct and complete.

CCDC-750249 (for **2**) and -750250 (for **1**) contain the supplementary crystallographic data for this paper. These data can be obtained free of charge from The Cambridge Crystallographic Data Centre via www.ccdc.cam.ac.uk/data_request/cif.

Supporting Information (see also the footnote on the first page of this article): Figures S1–S6: ^1H, $^{13}C\{^1H\}$, HSQC, DEPT NMR spectra of $[Pb_9Ir(cod)]^{3-}$ (**2**) and $^{13}C\{^1H\}$ NMR spectrum of $[Sn_9Ir(cod)]^{3-}$ (**1**).

Acknowledgments

This material is based upon work supported by the National Science Foundation (grant number CHE0401850) and by the Department of Energy (DOE) Hydrogen Fuel Initiative (HFI) (grant number DE-FG02-05ER15731).

---

[1] T. F. Fassler, S. D. Hoffmann, *Angew. Chem. Int. Ed.* **2004**, *43*, 6242–6247.

[2] M. J. Moses, J. C. Fettinger, B. W. Eichhorn, *Inorg. Chem.* **2007**, *46*, 1036–1038.

[3] E. N. Esenturk, J. Fettinger, B. Eichhorn, *J. Am. Chem. Soc.* **2006**, *128*, 9178–9186.

[4] A. H. H. Chang, W. C. Ermler, R. M. Pitzer, *J. Chem. Phys.* **1991**, *94*, 5004–5010.

[5] Z.-M. Sun, H. Xiao, J. Li, L.-S. Wang, *J. Am. Chem. Soc.* **2007**, *129*, 9560–9561.

[6] F. S. Kocak, P. Zavalij, Y.-F. Lam, B. W. Eichhorn, *Inorg. Chem.* **2008**, *47*, 3515–3520.

[7] S. Scharfe, T. F. Fassler, S. Stegmaier, S. D. Hoffmann, K. Ruhland, *Chem. Eur. J.* **2008**, *14*, 4479–4483.

[8] J. M. Goicoechea, S. C. Sevov, *Organometallics* **2006**, *25*, 4530–4536.

[9] B. Kesanli, J. Fettinger, D. R. Gardner, B. Eichhorn, *J. Am. Chem. Soc.* **2002**, *124*, 4779–4786.

[10] B. B. Zhou, M. S. Denning, D. L. Kays, J. M. Goicoechea, *J. Am. Chem. Soc.* **2009**, *131*, 2802–2803.

[11] I. Silaghi-Dumitrescu, B. King, *Studia Universitatis Babes-Bolyai Chemia* **2008**, *53*, 83–88.

[12] J. Q. Wang, S. Stegmaier, T. F. Fassler, *Angew. Chem. Int. Ed.* **2009**, *48*, 1998–2002.

[13] N. Korber, *Angew. Chem. Int. Ed.* **2009**, *48*, 3216–3217.

[14] J. Wang, X. Chen, J. H. Liu, *J. Phys. Chem. A* **2008**, *112*, 8868–8876.

[15] K. Wade, *Chem. Br.* **1975**, *11*, 177–183.

[16] B. Kesanli, J. Fettinger, B. Eichhorn, *Chem. Eur. J.* **2001**, *7*, 5277–5285.

[17] J. Campbell, H. P. A. Mercier, H. Franke, D. P. Santry, D. A. Dixon, G. J. Schrobilgen, *Inorg. Chem.* **2001**, *40*, 86–107.

[18] L. Yong, S. D. Hoffmann, T. F. Fassler, *Eur. J. Inorg. Chem.* **2005**, 3663–3669.

[19] B. B. Zhou, M. S. Denning, T. A. D. Chapman, J. M. Goicoechea, *Inorg. Chem.* **2009**, *48*, 2899–2907.

[20] C. Schenk, A. Schnepf, *Chem. Commun.* **2009**, 3208–3210.

[21] C. Xu, T. H. Baum, A. L. Rheingold, *Chem. Mater.* **1998**, *10*, 2329–2331.

[22] M. Martin, E. Sola, O. Torres, P. Plou, L. A. Oro, *Organometallics* **2003**, *22*, 5406–5417.

[23] J. Cipot, C. M. Vogels, R. McDonald, S. A. Westcott, M. Stradiotto, *Organometallics* **2006**, *25*, 5965–5968.

[24] J. Cipot, R. McDonald, M. J. Ferguson, G. Schatte, M. Stradiotto, *Organometallics* **2007**, *26*, 594–608.

[25] H. M. Lee, T. Jiang, E. D. Stevens, S. P. Nolan, *Organometallics* **2001**, *20*, 1255–1258.

[26] S. L. James, D. M. P. Mingos, X. L. Xu, A. J. P. White, D. J. Williams, *J. Chem. Soc., Dalton Trans.* **1998**, 1335–1340.

[27] M. W. D. L. Brown, R. Gillian, M. Webster, *Dalton Trans.* **2006**, 4039–4046.

Received: October 7, 2009